Supporting Online Material for

Topographical and Temporal Diversity of the Human Skin Microbiome

Elizabeth A. Grice, Heidi H. Kong, Sean Conlan, Clayton B. Deming, Joie Davis, Alice C. Young, NISC Comparative Sequencing Program, Gerard G. Bouffard, Robert W. Blakesley, Patrick R. Murray, Eric D. Green, Maria L. Turner, Julia A. Segre*

*To whom correspondence should be addressed. E-mail: jsegre@nhgri.nih.gov

Published 29 May 2009, *Science* **324**, 1190 (2009)
DOI: 10.1126/science.1171700

This PDF file includes:

SUPPORTING ONLINE MATERIALS

Methods

Subject recruitment and sampling: To analyze intrapersonal variation between different skin sites, we selected 20 sites (Table 1), including sebaceous, dry, and moist body regions and comparable areas for sites with bilateral symmetry. The study protocol was approved by the NHGRI Institutional Review Board (08-HG-0059) and all subjects gave written informed consent. We obtained samples from ten healthy volunteers, including males and females ages 20-41 with different self-reported ethnicities, no history of chronic medical conditions or dermatologic diseases, and no active infections. To evaluate temporal variation, 5 of the 10 subjects were re-sampled 4-6 months after initial skin sampling. Skin preparation included using only Dove soap for hygiene for 7 days, avoiding topical antiseptics for 7 days, and avoiding all washing for 24 hours prior to sampling. Exclusion criteria included use of systemic antibiotics within 6 months of sampling. After obtaining medical and medication history, a complete dermatologic examination was performed. Study personnel changed sterile gloves before each sample collection to minimize sample cross-contamination. Samples were collected from non-overlapping regions of the sites, with no prior cleaning or preparation of the skin surface. Swabs were obtained from 4-cm^2 areas using cotton tipped applicators (CTA) (Medline Industries, Mundelstein, IL; #MDS202000) soaked in enzymatic lysis buffer (20 mM Tris pH 8, 2 mM EDTA, and 1.2% Triton X-100). Superficial skin scrapings were obtained from a 4-cm^2 area with a sterile disposable #15 blade. Skin scrapings were removed from blades using CTAs moistened in enzymatic lysis buffer. Negative controls of mock swabs and scrapings were collected and analyzed for each sampling. All clinical samples were stored at -80°C until further processing.

DNA extraction and purification: All biological specimens were first incubated in a preparation of enzymatic lysis buffer (20 mM Tris, pH 8.0, 2 mM EDTA, 1.2% Triton X-100) and lysozyme (20 mg/mL) for 30 minutes at 37°C. The standard protocol for lysing gram-positive

bacterial cells of the Invitrogen PureLink Genomic DNA kit (Carlsbad, CA; #K1820-02) was followed for all subsequent steps. Purified genomic DNA was resuspended in 50 µl of PureLink Genomic Elution Buffer and stored at -20°C.

PCR amplification, cloning, and sequencing of 16S rRNA genes: 16S rRNA genes were amplified from purified genomic DNA using the primers 8F (5'-AGAGTTTGATCCTGGCTCAG-3') and 1391R (5'-GACGGGCGGTGTGTRCA-3') (*1*). Takara Taq DNA Polymerase Hot-Start kit was used for amplifications (Takara Bio USA, Madison WI; #TAK R007A). For each 25-µl reaction, conditions were as follows: 2.5 µl 10X Buffer with $MgCl_2$, 4 µl dNTP mix (2.5 mM each), 0.5 µl each primer (20 µM, IDT, Coralville IA), 2 µl clinical genomic DNA, and 0.25 µl Takara HS Taq polymerase. For each DNA sample, 3 replicates were performed. Thermocycling was as follows: initial denaturation at 95°C for 5 minutes, followed by 25-30 cycles of a 30 second 95°C denaturation, 30 second annealing at 55°C, and 1.5 minute elongation at 72°C, all followed by a final extension of 10 minutes at 72°C. Cycle number was determined on a case-by-case basis, such that amplification was still in the linear range of the reaction when stopped, but sufficient PCR product for cloning was produced (usually 25-28 cycles). PCR products were then separated on an agarose gel, and bands corresponding to the ~1.3-kb product were extracted. Negative control (no template) PCR reactions were performed with each set of amplifications and in all cases did not produce an amplification product. PCR products were extracted using the Qiaquick Gel Extraction kit (Qiagen, Valencia CA; #28706), resuspended in 30 µl of Buffer EB, cloned into the pCR2.1-TOPO vector (Invitrogen, Carlsbad, CA) and resulting plasmids transformed per the manufacturer's protocol. At least 384 of the resulting bacterial colonies per ligation were picked, plasmid DNA was purified, and plasmid inserts were sequenced at NISC on an ABI 3730xl sequencer (Applied Biosystems Inc., Foster City CA) using M13 primers flanking the insert and a

universal internal primer at position 522 (5'-CAGCMGCCGCGGTAATWC). Clones were re-picked if the average Q20 read length was <300 bases or the pass rate was <50%.

Analysis Pipeline

Sequencing assembly, alignment, and chimera elimination. Traces were base called using Phred (v 0.990722.g), trimmed using Crossmatch and assembled for each clone using Phrap (v 0.990329) with the default parameters except force level was 9 and the mismatch penalty was -1 (*2, 3*). Overall assembly quality was assessed using a measure of cumulative error, the average probability of a base being miscalled, defined as:

$Error_{Cumulative} = (\sum 10^{-Qi/10}) / L$, where Q*i* = Phred score at position *i*; L = sequence length

The resulting assemblies and quality data were stored in an Oracle database along with descriptive data for each sample. Sequences were further screened against the human genome, classified using the RDP classifier (*4*), aligned using the Greengenes (*5*) NAST aligner (*6*) and chimera checked using the implementation of Bellerophon (v.3) at Greengenes (*7*) using default parameters. Sequences were omitted from further analysis if they had a cumulative error >0.02; or matched the human genome (E-value < 0.1); or were less than 1,250 base pairs long; or were flagged as putative chimeras. A total of 168,524 assemblies were generated. Of those, 1,679 were putative chimeras, 7,767 were short or were homologous to human sequence, and 32,161 were of low quality using the above standards. Sequences were assigned to taxonomy using the Ribosomal Database Project (RDP) naïve Bayesian classifier (*8*). A residual group of 187 non-chimeric sequences were unclassifiable.

Operational taxonomic unit clustering. OTUs were identified using the Distance-based Richness and OTU (DOTUR) software (*9*). Olsen-corrected distance matrices were calculated by importing non-chimeric NAST-aligned sequences into ARB (*10*). The Hugenholtz lane mask (lanemaskPH; included with Greengenes ARB database) was applied to exclude hypervariable regions. The resulting distance matrix was then analyzed in DOTUR to calculate OTUs using the furthest-neighbor algorithm and a similarity cutoff of 99%.

Diversity Estimation. The Shannon Diversity Index (*H'*) was calculated using DOTUR as follows:

$$H' = -\Sigma p_i \ln(p_i)$$

Where p_i is the relative abundance of the *i*th OTU. The Shannon Equitability Index ($E_{H'}$), which measures OTU evenness, was calculated separately using spreadsheet software as follows:

$$E_{H'} = H'/\ln(S)$$

*W*here p_i is the relative abundance of the *i*th OTU and *S* is the number of total OTUs at 99% similarity threshold.

Statistical comparison of clone libraries. The SONS program was used to compare clone libraries at a specific phylogenetic level of 99% OTU identity (*11*). Shared community membership was calculated as a Jaccard index value (Jclas column 16 output), which falls between 0 and 1: a value of 0 implies that the two communities do not share any OTUs and a value of 1 implies that the communities share all OTUs. Specifically,

$$J_{clas} = S_{12} / (S_1 + S_2 - S_{12})$$

Where S_1 and S_2 represent the number of OTUs observed in communities A and B.

Shared community structure was calculated as a Theta index value (θ_N; ThetaN column 20 output), which also falls between 0 and 1: a value of 1 implies identical community structure and a value of 0 implies dissimilar community structure. θ_N accounts for relative abundance of OTUs shared between communities A and B and thus measures shared community structure (*12*).

$$\theta_N = [\Sigma (X_i/n_{total}) \cdot \Sigma (Y_i/m_{total})] / [\sum (X_i/n_{total}) + \Sigma (Y_i/m_{total}) - [\Sigma (X_i/n_{total}) \cdot \Sigma (Y_i/m_{total})]$$

Where X_i and Y_i are the abundance of the i^{th} OTU in communities A and B and m_{total} and n_{total} represent total number of sequences sampled in A and B.

SUPPLEMENTARY REFERENCES

1. P. B. Eckburg *et al.*, *Science* **308**, 1635 (2005).
2. B. Ewing, P. Green, *Genome Res* **8**, 186 (1998).
3. B. Ewing, L. Hillier, M. C. Wendl, P. Green, *Genome Res* **8**, 175 (1998).
4. Q. Wang, G. M. Garrity, J. M. Tiedje, J. R. Cole, *Appl Environ Microbiol* **73**, 5261 (2007).
5. T. Z. DeSantis *et al.*, *Appl Environ Microbiol* **72**, 5069 (2006).
6. T. Z. DeSantis, Jr. *et al.*, *Nucleic Acids Res* **34**, W394 (2006).
7. T. Huber, G. Faulkner, P. Hugenholtz, *Bioinformatics* **20**, 2317 (2004).
8. J. R. Cole *et al.*, *Nucleic Acids Res* **35**, D169 (2007).
9. P. D. Schloss, J. Handelsman, *Appl Environ Microbiol* **71**, 1501 (2005).
10. W. Ludwig *et al.*, *Nucleic Acids Res* **32**, 1363 (2004).
11. P. D. Schloss, J. Handelsman, *Appl Environ Microbiol* **72**, 6773 (2006).
12. J. C. Yue, M. K. Clayton, *Commun. Stat. Theor. M.* **34**, 2123 (2005).

Figures and Tables

Figure S1: The 20 selected skin sites and their location on the human body. The sites represent three microenvironments: sebaceous (blue), dry (red), and moist (green).

Figure S2: Taxonomic profile for each healthy volunteer at each site. Y-axis represents relative abundance. See Figure S1 for key to site codes on x-axis. Superscripts on taxon name indicate phylum: 1-Actinobacteria; 2-Firmicutes; 3-Proteobacteria; 4-Bacteroidetes.

Figure S3: Complexity of bacterial communities colonizing skin sites. A. Median taxonomic richness of sites as measured by observed OTUs at 99% similarity threshold. B. Median taxonomic evenness, or the relative distribution of sequences across OTUs, of sites as measured by the Shannon equitability index. Error bars represent median absolute deviation. See Figure S1 for key to site codes displayed on the X-axis.

Figure S4: Intrapersonal and interpersonal similarity of antecubital fossa, axilla, and volar forearm. Bars represent the mean of pair-wise values calculated for each healthy volunteer. Error bars represent the standard error of the mean. * indicates significance by one-tailed paired *t* test, $P < 0.05$. See Table S2 for index and error values.

Figure S5: Similarity of swabs and scrapes. Intrapersonal sample variation is less than interpersonal variation for A. antecubital fossa, B. axilla, C. occiput, and D. volar forearm. $P<0.003$ by one-tailed *t* test for both Jaccard and Theta indices and for all four sites Error bars represent the standard error of the mean.

Figure S6: Longitudinal stability of the skin microbiome for each re-sampled volunteer. Y-axis represents relative abundance. Healthy volunteer (HV) ID is at the right of each chart. See Figure S1 for key to skin sites on X-axis. A "-1" after the site abbreviation indicates the initial visit and a "-2" indicates the follow-up visit 4-6 months after the first sampling. Superscripts on taxon name indicate phylum: 1-Actinobacteria; 2-Firmicutes; 3-Proteobacteria; 4-Bacteroidetes.

Table S1: Number of sequences analyzed per healthy volunteer at each site and each sampling method. Does not include chimeric and low-quality sequences that were removed before analysis. A "-1" after the healthy volunteer identification number indicates the initial visit and a "-2" indicates the follow-up visit 4-6 months after the first sampling. Notation with site codes (see Figure S1 for legend) indicate: Sc=scrape, Sw=swab, L=left, R=right.

Table S2: Abundanceof major bacterial groups when sites are clustered into microenvironments (sebaceous, moist, or dry).

Table S3: Shared community membership (measured by the Jaccard index) and community structure (measured by the Theta index) of the symmetric left/right skin sites. The controls are calculated by averaging interpersonal index scores for the same site. SE is standard error.

Table S4: Shared community membership (measured by Jaccard index) and community structure (measured by Theta index) of scrapes and swabs of the same sites obtained from the same volunteer. The controls are calculated by averaging interpersonal index scores for the same site. SE is standard error.

Table S5: Shared community membership (measured by Jaccard index) and community structure (measured by Theta index) comparing interpersonal variation at each site. SE is standard error.

Tables S6 (A-C): Shared community membership (measured by median Jaccard index) and community structure (measured by median Theta index) of sites associated with A. atopic dermatitis, B. psoriasis, and C. the nare, a site that is not cornified like the other 19 sites. The three highest pair-wise scores are highlighted in yellow.

Table S7: Longitudinal shared community membership (measured by Jaccard index) and community structure (measured by Theta index) of sites. When considering all sites together, 4 of the 5 healthy volunteers re-sampled were found to be significantly more like themselves over time then they were like other volunteers (Jaccard index: P=0.037, <0.001, <0.001, and 0.008 and Theta index: P<0.001, 0.003, <0.001, 0.002 for volunteers 1, 3, 4, and 6, respectively). Controls are calculated by averaging interpersonal variation of the indices.

Grice *et al*, Figure S1

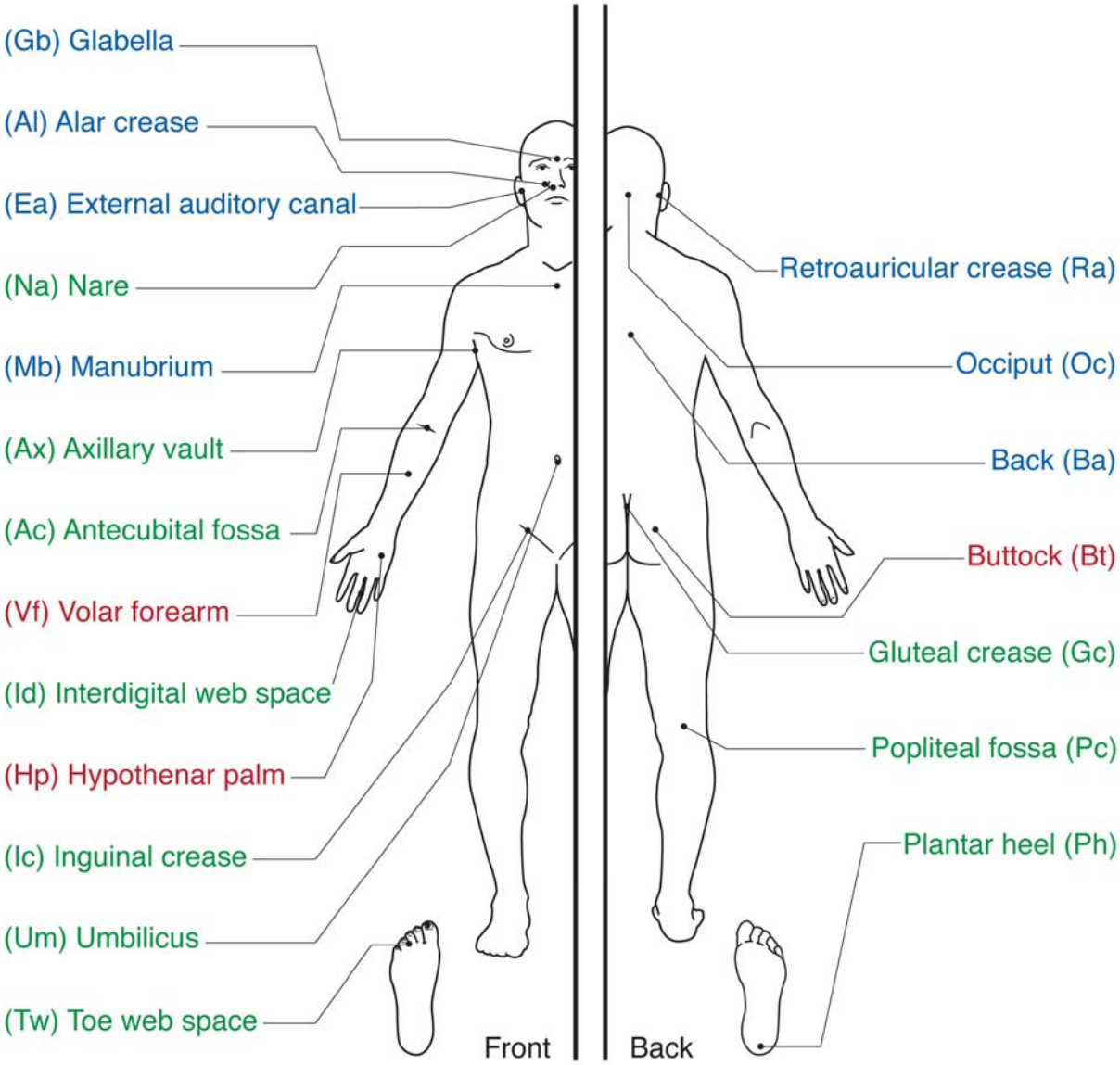

Grice *et al*, Figure S2

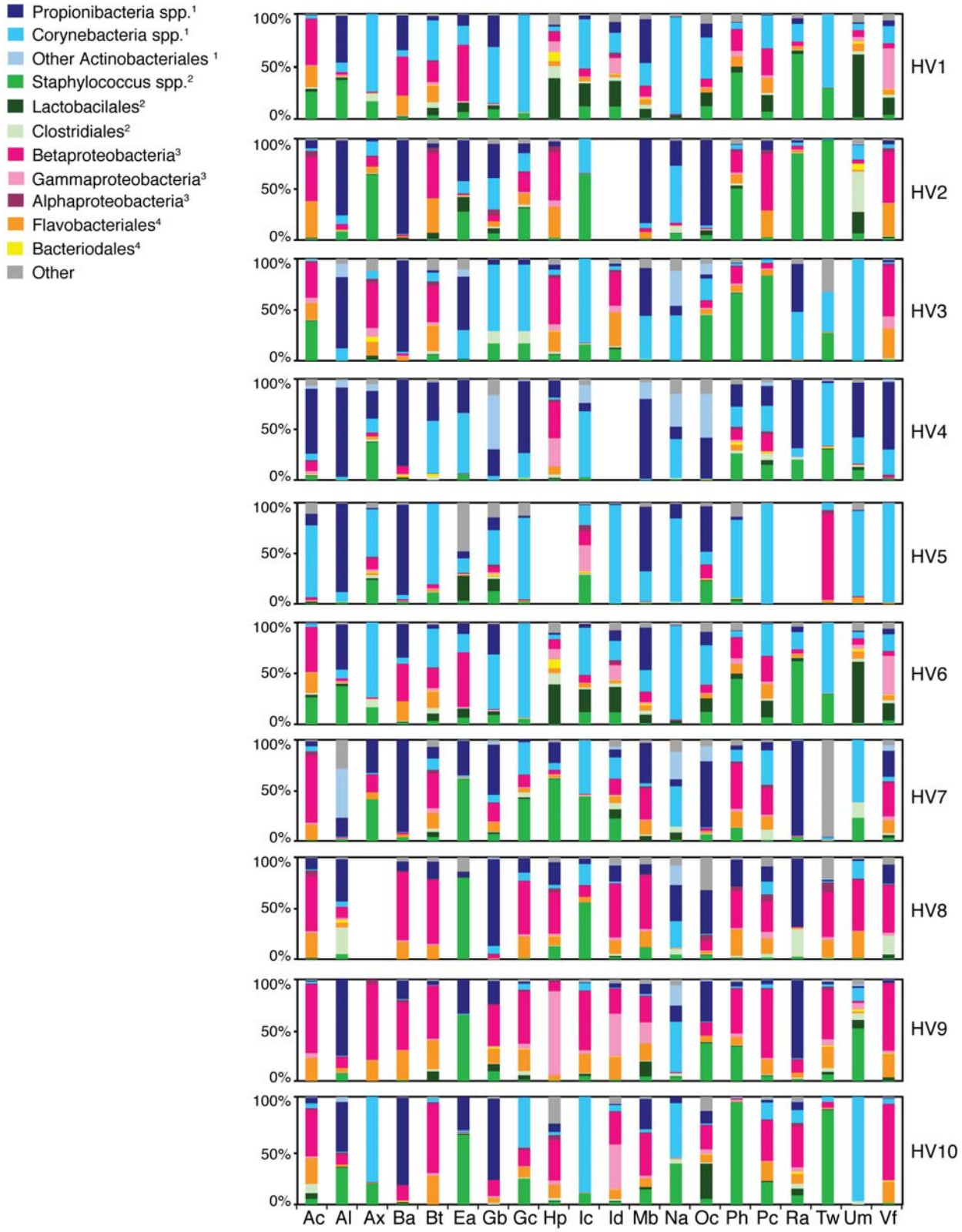

Grice *et al*, Figure S3

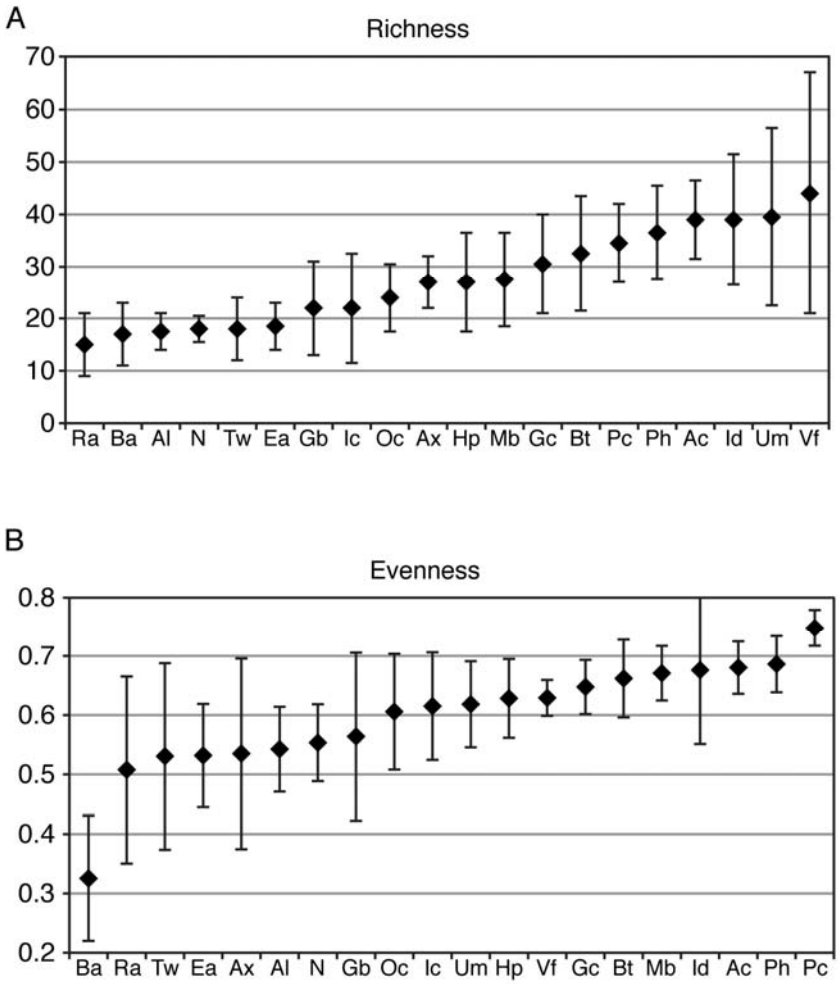

Grice *et al*, Figure S4

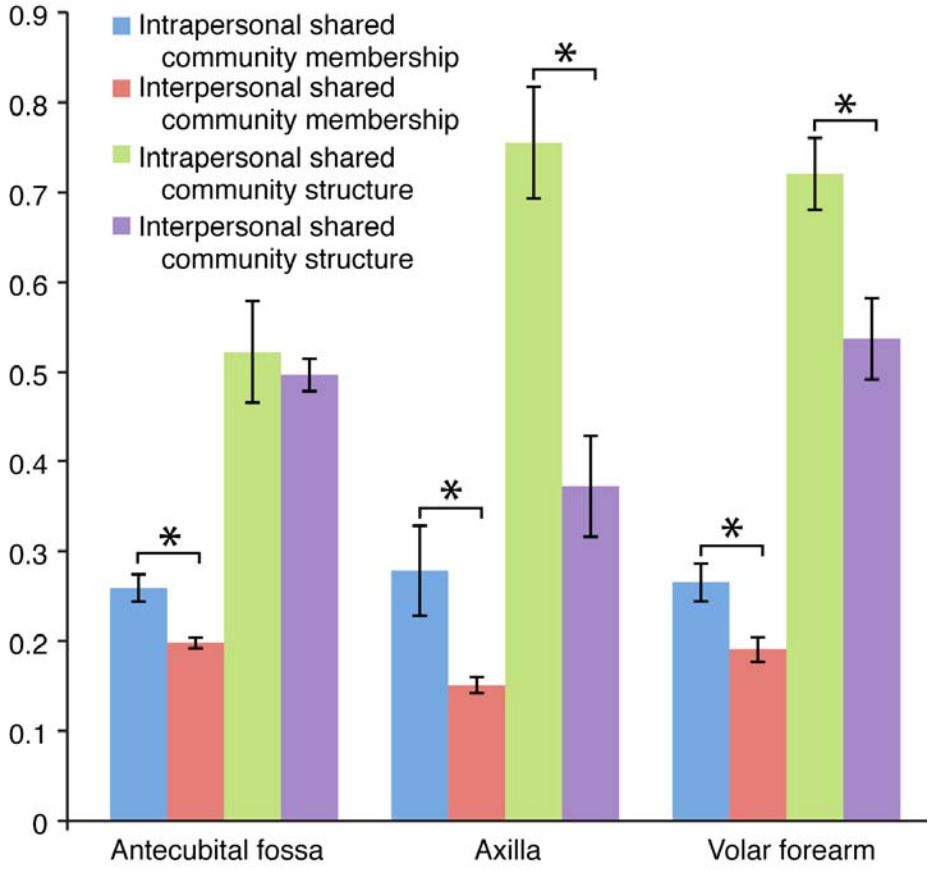

Grice *et al*, Figure S5

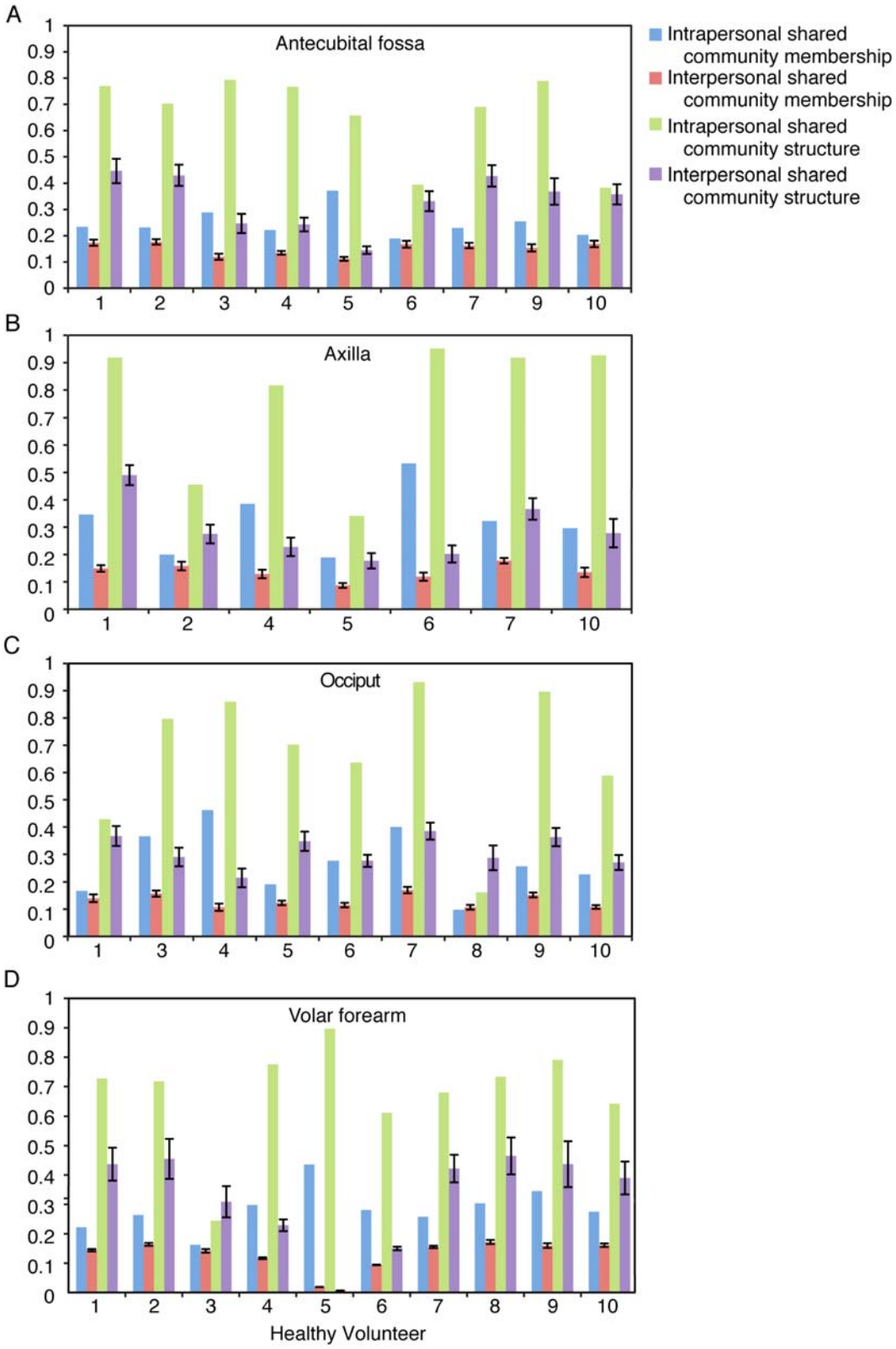

Grice *et al*, Figure S6

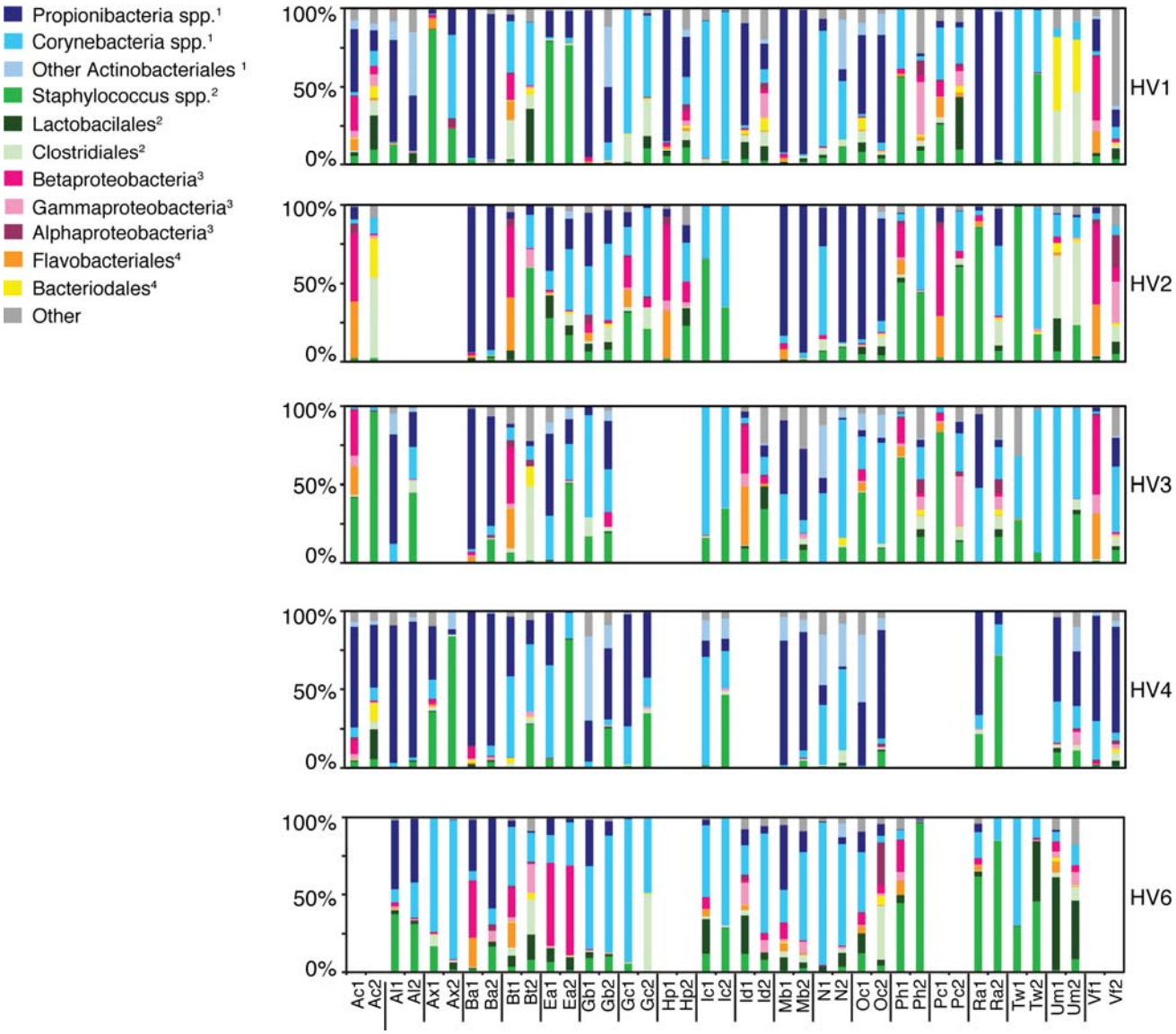

Grice *et al*, Table S1

site	HV1-1	HV1-2	HV2-1	HV2-2	HV3-1	HV3-2	HV4-1	HV4-2	HV5	HV6-1	HV6-2	HV7	HV8	HV9	HV10
AcLSc	317	0	320	550	0	278	0	291	0	270	208	301	44	347	264
AcRSc	278	334	304	283	285	297	270	194	212	295	0	655	303	302	254
AcRSw	338	282	303	258	199	245	253	273	315	269	250	312	0	296	269
AlRSc	330	301	304	0	287	349	342	207	250	314	211	288	364	336	276
AxLSc	373	344	283	0	0	0	0	247	356	679	195	298	0	0	326
AxRSc	350	317	236	0	258	0	271	328	297	349	284	335	0	558	311
AxRSw	375	342	278	0	0	0	206	319	270	333	215	293	0	0	317
BaCSc	305	302	354	200	180	291	296	259	673	334	312	338	297	263	289
BtRSc	326	347	308	268	308	317	429	316	350	280	282	304	290	331	198
EaRSw	342	352	282	666	271	322	207	284	272	326	338	334	335	340	318
GbCSc	295	318	242	270	287	307	297	277	263	345	272	318	290	272	240
GcCSc	311	345	305	267	294	321	451	240	354	359	255	339	279	286	251
HpRSc	294	344	355	294	290	0	274	0	0	341	0	321	170	276	536
IcRSc	321	355	353	356	337	349	208	192	282	273	290	519	275	602	319
IdRSc	345	331	0	303	299	339	0	214	313	310	211	340	278	308	328
MbCSc	525	302	210	357	197	314	164	321	280	279	267	264	308	293	312
NRSw	326	318	522	319	233	337	287	62	292	339	279	275	319	326	269
OcCSc	352	334	0	262	180	297	214	280	325	329	269	348	291	586	231
OcCSw	325	280	491	317	241	296	210	280	296	329	237	324	321	277	239
PcRSc	333	271	341	252	223	309	194	0	220	280	0	339	277	319	209
PhRSc	335	333	299	343	310	325	141	0	263	306	194	305	269	319	327
RaRSc	286	357	893	260	314	328	169	154	0	337	318	319	191	280	291
TwRSc	355	365	363	296	213	360	244	269	295	342	274	299	305	499	334
UmCSw	303	299	346	269	331	318	304	252	354	322	271	325	540	336	313
VfLSc	323	0	326	243	0	161	0	333	0	314	249	297	250	527	255
VfRSc	318	355	338	218	208	168	206	239	345	274	0	323	339	349	321
VfRSw	367	0	341	566	247	274	282	219	328	281	215	337	270	322	318

Grice *et al*, Table S2

SEBACEOUS SITES

	HV1	HV2	HV3	HV4	HV5	HV6	HV7	HV8	HV9	HV10	total
Propionibacterium	1944	1364	773	1082	1208	612	1477	825	1071	809	11165
Staphylococcus	384	915	249	12	211	469	301	348	612	400	3901
Corynebacterium	27	185	624	357	337	662	45	41	18	56	2352
Betaproteobacteria	27	81	34	21	100	399	171	456	492	435	2216
Other	105	35	101	189	212	107	142	283	23	81	1278
Unclassified Actinomycetales	91	2	103	400	0	0	250	6	12	16	880
Flavobacteriales	20	70	29	4	4	122	97	135	250	106	842
Lactobacillales	50	87	2	6	104	173	20	7	74	187	710
Clostridiales	55	12	40	1	8	23	12	127	8	23	309
Gammaproteobacteria	1	2	8	3	12	19	8	20	64	47	184
Alphaproteobacteria	2	22	1	3	17	4	10	49	19	26	153
Bacteroidales	54	1	0	8	9	3	0	7	4	10	96

MOIST SITES

	HV1	HV2	HV3	HV4	HV5	HV6	HV7	HV8	HV9	HV10	total
Corynebacterium	1128	232	599	527	1379	1127	630	125	96	727	6570
Betaproteobacteria	116	466	324	81	327	291	571	797	1797	339	5109
Staphylococcus	616	1007	686	264	174	484	612	173	191	827	5034
Flavobacteriales	98	275	184	14	24	152	201	352	599	160	2059
Propionibacterium	360	92	25	527	49	49	190	252	71	23	1772
Other	111	39	120	71	128	60	340	114	46	28	1057
Gammaproteobacteria	14	9	60	12	83	73	28	50	229	148	706
Lactobacillales	54	15	15	15	14	205	41	9	47	20	435
Clostridiales	94	17	44	27	12	56	80	22	36	30	418
Alphaproteobacteria	9	48	23	16	38	16	36	81	63	17	347
Unclassified Actinomycetales	16	0	1	75	0	0	9	11	9	4	125
Bacteroidales	13	1	13	16	8	1	2	0	9	1	64

DRY SITES

	HV1	HV2	HV3	HV4	HV5	HV6	HV7	HV8	HV9	HV10	total
Betaproteobacteria	189	479	344	101	12	96	217	404	430	556	2828
Corynebacterium	116	13	43	278	615	167	69	7	1	40	1349
Flavobacteriales	89	324	196	22	13	74	93	55	189	181	1236
Propionibacterium	324	43	26	349	3	32	176	151	24	41	1169
Gammaproteobacteria	23	23	53	77	4	148	27	18	242	28	643
Staphylococcus	40	19	39	6	41	22	218	26	2	20	433
Other	32	28	53	20	3	58	45	44	7	139	429
Lactobacillales	20	23	3	4	0	197	26	12	42	5	332
Clostridiales	86	1	18	23	2	61	17	64	7	13	292
Alphaproteobacteria	10	48	27	10	2	7	17	17	4	28	170
Bacteroidales	3	0	3	14	0	33	1	1	1	4	60
Unclassified Actinomycetales	6	0	1	5	0	0	16	0	2	0	30

Grice *et al*, Table S3

	Healthy Volunteer	Jaccard Index	Jaccard Index Control	Jaccard Control SE	Theta Index	Theta Index Control	Theta Control SE
Antecubital Fossa	1	0.265	0.191	0.009	0.717	0.511	0.034
	2	0.275	0.193	0.008	0.503	0.494	0.039
	6	0.306	0.213	0.008	0.663	0.558	0.035
	7	0.260	0.218	0.011	0.477	0.521	0.040
	9	0.192	0.179	0.013	0.407	0.456	0.045
	10	0.258	0.196	0.012	0.367	0.440	0.045
Axilla	1	0.186	0.175	0.026	0.619	0.525	0.089
	2	0.429	0.149	0.026	0.883	0.400	0.092
	6	0.326	0.119	0.026	0.718	0.182	0.065
	7	0.154	0.146	0.028	0.637	0.349	0.081
	10	0.296	0.165	0.028	0.919	0.404	0.091
Volar forearm	1	0.176	0.178	0.013	0.644	0.579	0.046
	2	0.208	0.175	0.014	0.805	0.533	0.046
	6	0.306	0.124	0.012	0.520	0.274	0.044
	7	0.328	0.212	0.017	0.783	0.598	0.050
	8	0.289	0.222	0.019	0.704	0.586	0.050
	9	0.259	0.215	0.020	0.807	0.619	0.049
	10	0.292	0.213	0.018	0.782	0.571	0.047

Grice *et al*, Table S4

	Healthy Volunteer	Jaccard Index	Jaccard Index Control	Jaccard Control SE	Theta Index	Theta Index Control	Theta Control SE
Antecubital Fossa	1	0.234	0.174	0.012	0.769	0.447	0.046
	2	0.232	0.177	0.010	0.702	0.430	0.040
	1	0.289	0.120	0.011	0.793	0.247	0.036
	2	0.222	0.135	0.007	0.767	0.243	0.026
	3	0.372	0.112	0.008	0.657	0.145	0.015
	4	0.190	0.168	0.013	0.395	0.332	0.038
	7	0.230	0.163	0.010	0.691	0.428	0.040
	9	0.255	0.154	0.014	0.789	0.369	0.051
	10	0.204	0.169	0.012	0.383	0.358	0.039
Axilla	1	0.346	0.149	0.012	0.916	0.490	0.036
	2	0.200	0.158	0.016	0.453	0.275	0.034
	2	0.385	0.129	0.016	0.814	0.228	0.034
	3	0.189	0.087	0.009	0.338	0.177	0.028
	4	0.533	0.119	0.015	0.949	0.202	0.032
	7	0.323	0.177	0.010	0.916	0.366	0.039
	10	0.296	0.135	0.017	0.924	0.278	0.052
Occiput	1	0.167	0.140	0.014	0.431	0.367	0.037
	1	0.366	0.157	0.011	0.799	0.290	0.034
	2	0.462	0.107	0.013	0.862	0.214	0.034
	3	0.191	0.123	0.008	0.705	0.348	0.035
	4	0.276	0.115	0.008	0.639	0.276	0.022
	7	0.400	0.170	0.011	0.934	0.385	0.031
	6	0.098	0.107	0.008	0.164	0.287	0.045
	9	0.256	0.152	0.009	0.899	0.363	0.033
	10	0.226	0.108	0.007	0.591	0.270	0.027
Volar Forearm	1	0.222	0.144	0.004	0.728	0.437	0.056
	2	0.264	0.164	0.005	0.719	0.455	0.068
	1	0.163	0.142	0.006	0.245	0.309	0.053
	2	0.298	0.117	0.003	0.776	0.229	0.020
	3	0.436	0.019	0.000	0.898	0.007	0.000
	4	0.281	0.094	0.001	0.611	0.150	0.006
	7	0.258	0.155	0.004	0.681	0.422	0.047
	6	0.304	0.172	0.007	0.734	0.465	0.063
	9	0.346	0.160	0.008	0.792	0.437	0.078
	10	0.275	0.161	0.006	0.643	0.390	0.056

Grice *et al*, Table S5

	Jaccard Index		Theta Index	
	average	SE	average	SE
Alar crease	0.228	0.009	0.549	0.033
Antecubital fossa	0.177	0.012	0.429	0.041
Axilla	0.121	0.011	0.217	0.022
Back	0.195	0.008	0.564	0.042
Buttock	0.158	0.011	0.371	0.045
Ext. auditory canal	0.176	0.008	0.363	0.035
Glabella	0.133	0.008	0.403	0.040
Gluteal crease	0.149	0.010	0.396	0.033
Hypothenar palm	0.136	0.009	0.307	0.044
Inguinal crease	0.174	0.010	0.359	0.037
Interdigital web space	0.119	0.012	0.243	0.033
Manubrium	0.186	0.009	0.454	0.023
Nare	0.215	0.008	0.483	0.035
Occiput	0.147	0.009	0.258	0.027
Plantar heel	0.170	0.015	0.348	0.036
Popliteal fossa	0.143	0.012	0.387	0.036
Retroauricular crease	0.154	0.012	0.384	0.042
Toeweb	0.111	0.012	0.267	0.035
Umbilicus	0.057	0.008	0.114	0.023
Volar forearm	0.154	0.020	0.371	0.067

Grice *et al*, Table S6

A

Pairwise comparison		Median Jaccard	Median Theta
Antecubital Fossa	Alar Crease	0.181	0.599
	Axilla	0.164	0.489
	Back	0.169	0.636
	Buttock	0.265	0.658
	Ext Auditory Canal	0.098	0.170
	Glabella	0.199	0.607
	Gluteal Crease	0.200	0.440
	Hypothenar Palm	0.195	0.538
	Inguinal Crease	0.159	0.339
	Interdigital Web Space	0.197	0.502
	Manubrium	0.268	0.669
	Nare	0.095	0.205
	Occiput	0.183	0.473
	Popliteal Fossa	0.224	0.601
	Plantar Heel	0.254	0.656
	Retroauricular Crease	0.209	0.536
	Toeweb	0.143	0.308
	Umbilicus	0.119	0.124
	Volar Forearm	0.285	0.666
Popliteal Fossa	Antecubital Fossa	0.234	0.576
	Alar Crease	0.175	0.384
	Axilla	0.143	0.430
	Back	0.143	0.395
	Buttock	0.220	0.567
	Ext Auditory Canal	0.124	0.166
	Glabella	0.177	0.404
	Gluteal Crease	0.249	0.589
	Hypothenar Palm	0.175	0.401
	Inguinal Crease	0.181	0.390
	Interdigital Web Space	0.205	0.468
	Manubrium	0.183	0.499
	Nare	0.101	0.181
	Occiput	0.146	0.189
	Plantar Heel	0.190	0.523
	Retroauricular Crease	0.247	0.470
	Toeweb	0.128	0.358
	Umbilicus	0.130	0.372
	Volar Forearm	0.233	0.598
Retroauricular Crease	Antecubital Fossa	0.209	0.536
	Alar Crease	0.317	0.637
	Axilla	0.140	0.128
	Back	0.211	0.395
	Buttock	0.153	0.375
	Ext Auditory Canal	0.180	0.595
	Glabella	0.214	0.757
	Gluteal Crease	0.169	0.409
	Hypothenar Palm	0.163	0.150
	Inguinal Crease	0.133	0.344
	Interdigital Web Space	0.152	0.419
	Manubrium	0.234	0.644
	Nare	0.216	0.473
	Occiput	0.200	0.489
	Popliteal Fossa	0.247	0.470
	Plantar Heel	0.143	0.317
	Toeweb	0.148	0.409
	Umbilicus	0.070	0.121
	Volar Forearm	0.160	0.501

B

Pairwise comparison		Median Jaccard	Median Theta
Umbilicus	Antecubital Fossa	0.123	0.137
	Alar Crease	0.115	0.147
	Axilla	0.075	0.139
	Back	0.124	0.158
	Buttock	0.138	0.160
	Ext Auditory Canal	0.053	0.038
	Glabella	0.130	0.431
	Gluteal Crease	0.146	0.292
	Hypothenar Palm	0.111	0.068
	Inguinal Crease	0.158	0.409
	Interdigital Web Space	0.157	0.264
	Manubrium	0.172	0.221
	Nare	0.071	0.054
	Occiput	0.108	0.082
	Popliteal Fossa	0.105	0.270
	Plantar Heel	0.141	0.229
	Retroauricular Crease	0.070	0.292
	Toeweb	0.104	0.157
	Volar Forearm	0.149	0.244
Occiput	Antecubital Fossa	0.183	0.459
	Alar Crease	0.173	0.530
	Axilla	0.146	0.181
	Back	0.179	0.452
	Buttock	0.171	0.394
	Ext Auditory Canal	0.128	0.223
	Glabella	0.196	0.428
	Gluteal Crease	0.140	0.279
	Hypothenar Palm	0.165	0.339
	Inguinal Crease	0.158	0.224
	Interdigital Web Space	0.174	0.427
	Manubrium	0.196	0.565
	Nare	0.127	0.247
	Popliteal Fossa	0.146	0.189
	Plantar Heel	0.125	0.207
	Retroauricular Crease	0.200	0.489
	Toeweb	0.114	0.179
	Umbilicus	0.108	0.082
	Volar Forearm	0.174	0.401
Gluteal Crease	Antecubital Fossa	0.225	0.448
	Alar Crease	0.160	0.372
	Axilla	0.179	0.502
	Back	0.147	0.463
	Buttock	0.226	0.592
	Ext Auditory Canal	0.115	0.179
	Glabella	0.183	0.441
	Hypothenar Palm	0.129	0.177
	Inguinal Crease	0.210	0.572
	Interdigital Web Space	0.190	0.322
	Manubrium	0.200	0.564
	Nare	0.112	0.138
	Occiput	0.140	0.279
	Popliteal Fossa	0.249	0.589
	Plantar Heel	0.183	0.558
	Retroauricular Crease	0.169	0.409
	Toeweb	0.149	0.457
	Umbilicus	0.146	0.292
	Volar Forearm	0.193	0.435

Grice *et al*, Table S6 continued

C.

Pairwise comparison		Median Jaccard	Median Theta
Nare	Antecubital Fossa	0.104	0.205
	Alar Crease	0.292	0.568
	Axilla	0.066	0.127
	Back	0.142	0.152
	Buttock	0.078	0.076
	Ext. Auditory Canal	0.182	0.247
	Glabella	0.136	0.300
	Gluteal Crease	0.104	0.138
	Hypothenar Palm	0.094	0.128
	Inguinal Crease	0.126	0.165
	Interdigital Web Space	0.103	0.163
	Manubrium	0.195	0.325
	Occiput	0.128	0.274
	Popliteal Fossa	0.114	0.181
	Plantar Heel	0.098	0.140
	Retroauricular Crease	0.217	0.473
	Toeweb	0.081	0.110
	Umbilicus	0.090	0.090
	Volar Forearm	0.105	0.180

Grice *et al*, Table S7

Subsite	Healthy Volunteer	Jaccard Index	Theta Index	Jaccard Control	Theta control
Antecubital Fossa	1	0.202	0.367	0.150	0.333
	2	0.104	0.033	0.129	0.240
	3	0.139	0.287	0.102	0.165
	4	0.176	0.508	0.114	0.214
AlarCrease	1	0.143	0.570	0.195	0.548
	3	0.259	0.571	0.221	0.562
	4	0.273	0.689	0.189	0.307
	6	0.250	0.554	0.176	0.445
Axilla	1	0.122	0.783	0.107	0.271
	4	0.195	0.635	0.094	0.190
	6	0.129	0.257	0.078	0.114
Buttock	1	0.125	0.184	0.113	0.207
	2	0.058	0.023	0.108	0.234
	3	0.167	0.211	0.116	0.223
	4	0.188	0.530	0.101	0.166
	6	0.178	0.273	0.139	0.235
Back	1	0.172	0.769	0.173	0.533
	2	0.171	0.627	0.196	0.595
	3	0.200	0.614	0.183	0.574
	4	0.217	0.662	0.156	0.258
	6	0.120	0.289	0.181	0.448
Ext Auditory Canal	1	0.317	0.904	0.189	0.447
	2	0.254	0.529	0.143	0.353
	3	0.200	0.550	0.150	0.362
	4	0.200	0.594	0.171	0.372
	6	0.231	0.842	0.155	0.198
Glabella	1	0.177	0.653	0.144	0.449
	2	0.164	0.404	0.112	0.287
	3	0.205	0.696	0.129	0.394
	4	0.158	0.614	0.139	0.377
	6	0.182	0.870	0.093	0.240
Gluteal Crease	1	0.135	0.440	0.118	0.359
	2	0.179	0.486	0.149	0.393
	3	0.297	0.892	0.162	0.442
	4	0.283	0.657	0.148	0.276
	6	0.156	0.395	0.156	0.389
Inguinal Crease	1	0.283	0.856	0.199	0.400
	2	0.263	0.871	0.206	0.529
	3	0.184	0.369	0.203	0.481
	4	0.324	0.649	0.197	0.334
	6	0.136	0.522	0.197	0.479
Interdigital Web Space	1	0.096	0.258	0.099	0.239
	3	0.235	0.514	0.145	0.267
	6	0.128	0.298	0.097	0.170
Manubrium	1	0.167	0.842	0.185	0.535
	2	0.250	0.346	0.187	0.466
	3	0.200	0.487	0.179	0.422
	4	0.156	0.602	0.156	0.435
	6	0.143	0.402	0.130	0.323
Nare	1	0.200	0.775	0.222	0.552
	2	0.233	0.354	0.200	0.485
	3	0.235	0.789	0.214	0.523
	4	0.206	0.782	0.217	0.577
	6	0.255	0.807	0.185	0.371
Occiput	1	0.250	0.888	0.164	0.417
	3	0.216	0.654	0.132	0.209
	4	0.269	0.574	0.134	0.273
	6	0.082	0.081	0.108	0.168
Popliteal Fossa	1	0.143	0.276	0.127	0.296
	2	0.049	0.029	0.125	0.319
	3	0.130	0.368	0.119	0.321
PlantarHeel	1	0.061	0.099	0.137	0.230
	2	0.209	0.377	0.158	0.340
	3	0.203	0.288	0.165	0.291
	6	0.133	0.358	0.130	0.277
RetroauricularCrease	1	0.087	0.637	0.100	0.309
	2	0.087	0.066	0.120	0.312
	3	0.214	0.574	0.164	0.413
	4	0.250	0.619	0.156	0.386
	6	0.220	0.706	0.121	0.288
Toeweb	1	0.174	0.865	0.126	0.334
	2	0.185	0.522	0.135	0.290
	3	0.304	0.808	0.083	0.111
	4	0.122	0.353	0.109	0.311
	6	0.222	0.687	0.139	0.326
Umbilicus	1	0.192	0.463	0.047	0.067
	2	0.180	0.405	0.102	0.202
	3	0.125	0.514	0.068	0.091
	4	0.180	0.627	0.081	0.157
	6	0.206	0.418	0.071	0.117
VolarForearm	1	0.164	0.270	0.149	0.306
	2	0.055	0.023	0.109	0.236
	3	0.180	0.071	0.146	0.299
	4	0.149	0.638	0.121	0.186

Additional Authors, NISC Comparative Sequencing Program:

Beatrice Benjamin
Shelise Brooks
Grace Chu
Irina Chub
Holly Coleman
Lyudmila Dekhtyar
Tatyana Fuksenko
Maria Gestole
Michael Gregory
Xiaobin Guan
Jyoti Gupta
Natalie Gurson
Peggy Hall
Joel Han
Nancy Hansen
April Hargrove
Keisha Hines-Harris
Shiling Ho
Taccara Johnson
Richelle Legaspi
Sean Lovett
Maureen Madden
Quino Maduro
Cathy Masiello
Baishali Maskeri
Jenny McDowell
Casandra Montemayor
Jim Mullikin
Jerlil Myrick
Amber Palumbo
Morgan Park
Colleen Ramsahoye
Natalie Reddix-Dugue
Nancy Riebow
Karen Schandler
Brian Schmidt
Christina Sison
Lauren Smith
Sirintorn Stantripop
Pam Jacques Thomas